16th Australasian Fluid Mechanics Conference
Crown Plaza, Gold Coast, Australia
2-7 December 2007

Combination of Lighthill Acoustic Analogy and Stochastic Turbulence Modelling for Far-Field Acoustic Prediction

A. Ahmadzadegan and M. Tadjfar

Department of Aerospace Engineering, Amirkabir University of Technology, Tehran 15875-4413, Iran
Centre of Excellence in Computational Aerospace Engineering (AeroExcel)

Abstract

There are many approaches in determining the sound propagated from turbulent flows. Hybrid approaches, in which the turbulent noise source field is computed or modeled separately from the far-field calculation, are frequently used. To have a more feasible approach for basic estimation of sound propagation, cheaper methods can be developed using stochastic modeling of the turbulent fluctuations (turbulent noise source field).

In this paper, a simple and easy to use stochastic model for the generation of turbulent velocity fluctuations called continuous filter white noise (CFWN) model is used. This method is based on the use of classical Langevian-equation to model the details of fluctuating field superimposed on averaged computed quantities. The sound propagation due to the generated unsteady field is evaluated using Lighthill's acoustic analogy.

Our results are validated by comparing the directivity and the overall sound pressure level (OSPL) magnitudes with the available experimental results. Numerical results show reasonable agreement with the experiments, both in maximum directivity and magnitude of the OSPL.

Introduction

One of the major contributors to the overall aircraft's noise is due to its propulsive jet and fulfilling the governments' rules and regulations for quieter aircrafts demands its reduction [5]. This an arduous task to be done because of the noticeable inefficiency of turbulence as an acoustic source. When there is no solid surface in the flow field, quadrupole acoustic sources formed by the turbulent Reynolds stresses are responsible for generating sound [9]. Three hybrid methods may be used in computational aeroacoustics to study compressible jet flow. Each method has its own way for computing the near field turbulent flow and far field noise data [1]. First approach relies on direct numerical simulation (DNS) in which near field is computed by solving the full compressible Navier-Stokes equations. However the practical application of DNS is limited to low Reynolds numbers and simple geometries. Second approach uses the mean turbulent flow field computed using some turbulence modeling method combined with statistical source representation. In the third approach, the turbulent mean flow is computed as before, but the details of the turbulent fluctuation field are regenerated by stochastic or random-walk models. Lighthill's analogy or Kirchhoff's formulation [11] is used to estimate the far field jet noise.

In all of the mentioned methods, computing the near field has to be done first. Stochastic or random-walk models have proved to be a successful and flexible tool for simulating turbulent fluctuations in high-Reynolds-number turbulent flows. They can take account of inhomogeneities, unsteadiness or non-Gaussian distributions in the flow. They can also be used for complex flows [14].

Statistical methods are also used for subgrid scale modeling in LES simulations [2]. In this approach large eddies are solved numerically and small eddies are modeled stochastically.

More thorough descriptions of various computational aeroacoustic methods with more emphasis on the hybrid methods can be found in [12, 15].

In this paper, turbulent mean flow of a two dimensional, compressible, cold-jet at mach 0.56 is computed using RANS with 2 equation k-ε RNG model, then the mean-flow quantities are exported for use in the stochastic turbulence generation code to simulate the fluctuating velocities and finally computation of the far field noise is done using the aforementioned integration methods.

Characteristics of the Two-Dimensional Jet

We considered a free cold-jet configuration for applying our method because most of the references and available data in this field are about this problem. In a free cold-jet configuration due to very large velocity differences at the surface of discontinuity, large eddies are formed that cause intense lateral mixing. We know that in the zone of establishment of the jet, there is a core region that has constant velocity and very little turbulence. After the zone of establishment, diffusion of the momentum of ambient fluid reaches the centerline of the jet and the mean velocity on the symmetry line starts to decrease downstream thereafter. Figure 1 shows these properties of the free jet.

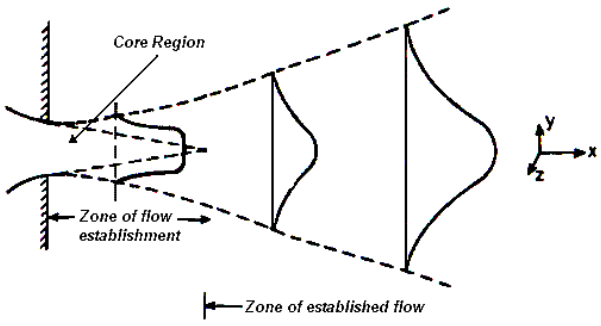

Figure 1. 2D free jet

The geometry and the computational domain of the two dimensional jet used for calculating the mean turbulent flow is shown in the figure 2.

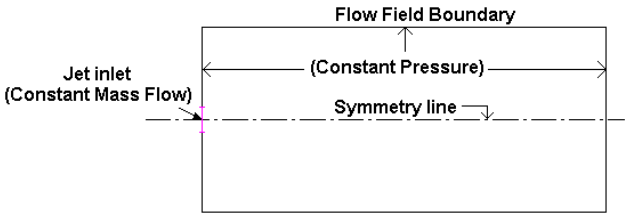

Figure 2. Geometry of the two dimensional jet

To compute the mean quantities of the turbulent flow, only half of the flow field above the symmetry line was considered, because the mean turbulent quantities are symmetrically distributed. All boundaries have constant pressure as their boundary condition. As a validation of our numerical results, the mean velocities are compared with the experimental data. The experimental data from reference [16] is given below:

$$\frac{\overline{u}_m}{U_0} = \frac{3.50}{\sqrt{x/b_0}} \qquad (1)$$

Where b_0 is the half of jet exit nozzle and U_0 is the jet velocity at the nozzle exit. In this study U_0=190 m/s and b_0=0.0005m. These experimental relations are from measurements in the fully developed region and are not valid in the potential region. As shown in figure 3, the computed mean velocity on the symmetry line lies on the experimental data in the fully developed region of the jet.

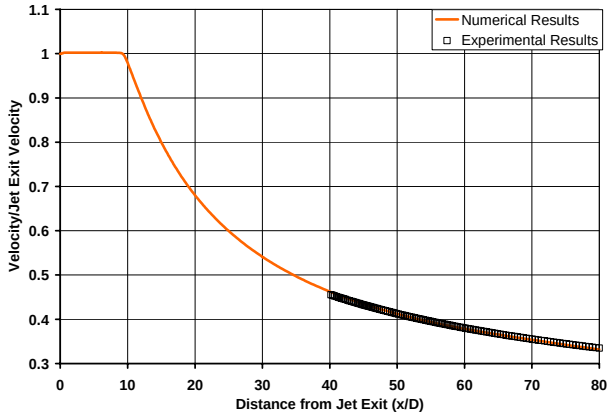

Figure 3. Comparison of numerical with experimental [16] velocities on the symmetry line

Another parameter that can be used to validate the numerical results is the velocity profile on the lines normal to the symmetry line. Experimental data curve fit appeared in reference [16] is given below:

$$\frac{\overline{u}}{\overline{u}_m} = e^{-a_0\left(\frac{y}{x}\right)^2} \qquad (2)$$

Where a_0 changes from 70.7 to 75.0, and also following the theoretical calculations presented in [6], we will find another equation:

$$\frac{\overline{u}}{\overline{u}_m} = 1 - \tanh^2 \xi \quad ; \quad \xi = \frac{\sigma y}{x} \qquad (3)$$

In this relation σ is a constant that have to be determined. Experimental investigations have reported this constant to be 7.67 [6].

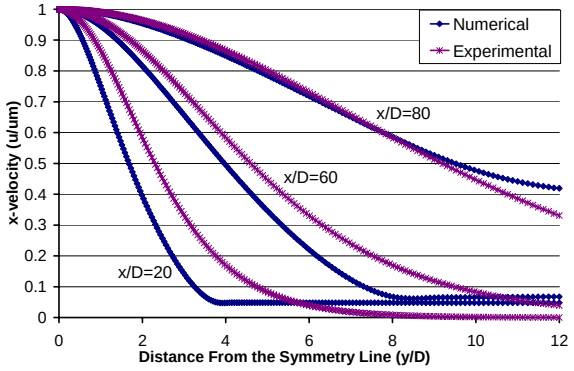

Figure 4. Comparison of the computed jet velocity profile normal to symmetry line with the experimental relation [16].

In figure 4, the comparison between the numerical results and the experimental data are presented. Note that in this figure all the velocities are non-dimentionalized with related velocity on the symmetry line of the jet so they all start from 1 and decrease as the distance from the symmetry line increases. As mentioned earlier the experimental relations have been given by interpolation of measurements in the fully developed region of the jet flow. So as we go further away from the jet exit, the numerical results better match the experimental data.

Description of the Stochastic Model

The turbulence fluctuations are random-like functions of space and time. In this study the continuous filter white noise (CFWN) model [4], which is based on the classical Langevian-equation [14] is used to simulate the instantaneous fluctuating velocity of the flow field.

$$\frac{du_i}{dt} = -\frac{u_i - \overline{u}_i}{T_I} + \left(\frac{2\overline{u_i'^2}}{T_I}\right)^{1/2} \zeta_i(t) \qquad (4)$$

Where, $\overline{u_i'^2}$ is the mean-square of the ith fluctuating velocity, and the summation convention on underlined indices is avoided. T_I is the Lagrangian integral time T_I=0.30k/ε. $\zeta_i(t)$ is a Gaussian vector white noise random function with spectral intensity $S_{ij}^n = \delta_{ij}/\pi$. This in the numerical method is determined as $G_i/\sqrt{\Delta t}$. G_i is a zero-mean unit variance independent Gaussian random number and has to be computed correctly in every time step, Δt, for the entire time range.

Equation 4 has to be solved for each direction of the flow field to obtain the velocity fluctuations in that direction. The information needed for arranging and solving equation 4 are mean velocities at each point of the flow field, kinetic energy of turbulence, k, rate of dissipation of kinetic energy of turbulence, ε, (All taken from the RANS solver), and the Gaussian random numbers G_i, which is generated using the polar form of the Box-Muller transformation. This is a fast and robust way to generate Gaussian random numbers [3]. Here, equation 4 is solved analytically and only the integration in the analytical solution was computed numerically. This way less computational error is introduced.

Since different equations are solved for each dimension, the generated turbulence field is not necessarily isotropic. Also note that this equation takes into account the intensity of local turbulence at each point ala the use of kinetic energy and dissipation rate in the formulation.

This technique has some advantages compared to other techniques. It provides correct turbulent intensities and accounts for the proper time scale of turbulence. More importantly the model leads to the correct magnitude of turbulent diffusivity for fluid point particles [4].

Validation of the Stochastic Model Used

To check the accuracy of the turbulence field generated using CFWN model, we computed the temporal power spectral density of the fluctuating velocity at the center of the jet. The ensemble average of the computed power at each frequency is plotted with respect to the frequency and presented in figure 5. The slope of the computed averaged spectrum is compared to the line with -5/3 slope. It is known that the slope of the spectrum in the inertial subrange region of the jet is -5/3 if we use logarithmic scale for both axes. As can be seen there is a good agreement between spectrum and -5/3 slope line which assures a correct procedure for the generation of turbulent velocity fluctuations.

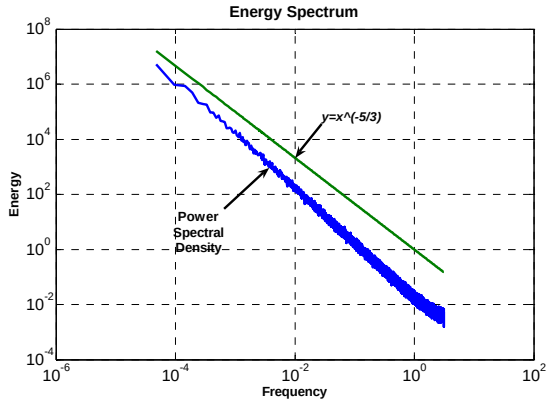

Figure 5. Comparison of the computed power spectral density with the -5/3 slope line

As shown in figure 3, there is a region right after the jet outlet that has the same velocity as the jet exit. This region is called the potential core of the jet and has a cone (in axi-symmetric jets) or wedge (in planar jets) shape. In this region we have potential flow because the momentum of the still medium next to jet has not diffused into it yet. This property of the jet velocity is shown in the velocity fluctuation contour of figure 6. Inside the core region of the jet, flow is not turbulent and therefore no velocity fluctuations are present.

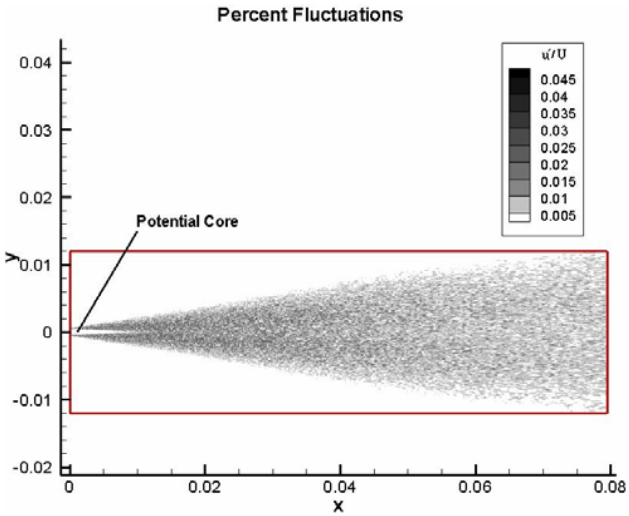

Figure 6. Velocity fluctuation contour showing no fluctuation in the core region of the jet

The CFWN method is categorized as a one point method, because the computation for velocity fluctuations in one point does not affect the velocity fluctuations of its adjacent points. As expected, this method does not generate realistic two-point correlations due to its single point nature.
The differential equation for modeling the turbulent fluctuations, equation 4, is just time dependent and no spatial correlation between adjacent points is possible. So this method can not satisfy the two point correlations present in the turbulent fields.

Evaluation of the Far Field Noise

In order to evaluate the far field noise emitted from the turbulent velocity distribution, we use the volume integration as prescribed by Lighthill's acoustic analogy [9]:

$$\rho - \rho_0 = \frac{1}{4\pi a_0^2}\frac{\partial^2}{\partial x_i \partial x_j}\int T_{ij}\left(\bar{y}, t - \frac{|\bar{x}-\bar{y}|}{a_0}\right)\frac{d\bar{y}}{|\bar{x}-\bar{y}|} \qquad (5)$$

Where T_{ij} is the Lighthill's quadrapole source that in most cases can be replaced by $\rho u_i u_j$. Note that T_{ij} is calculated at the retarded time, which is the time needed for the sound waves to travel the distance between source and observer positions. Here, all the discritizations is done using 4th order finite difference schemes [8].
Figure 7 presents a schematic of the far-field and the computational flow region. The overall sound pressure level, OSPL, of the sound at far field is computed along the perimeter of a half circle with the radius $\overline{X}$ (position vector).

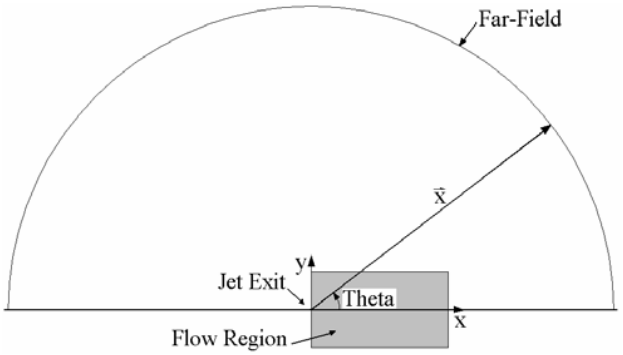

Figure 7. Schematic of the jet geometry and far-field region

Since we evaluate the exact form of the Lighthill's volume integral, it is possible to compute the contribution of the noise produced by any segment of the flow field separately. Far-field noise contribution produced by different segments of the jet flow is inspected. Different integration zones used in this study to evaluate the volume integral are given in figure 8.
Far from the source region of the jet where the acoustic fluctuations are governed by the linear wave equation, density and pressure fluctuations are related to each other as $p' = c_0^2 \rho'$, so we can easily compute the magnitude of the pressure fluctuations, using the computed density fluctuations values [7].
In figure 9, the overall sound pressure level, OSPL, as defined by equation 6, is shown for different integration regions of figure 8 on a half circle of radius $\overline{X}$ =200D.

$$OSPL = 20\log\left(\frac{p'_{rms}}{p_{ref}}\right) \quad where \quad p_{ref} = 2\times10^{-5}\,Pa \qquad (6)$$

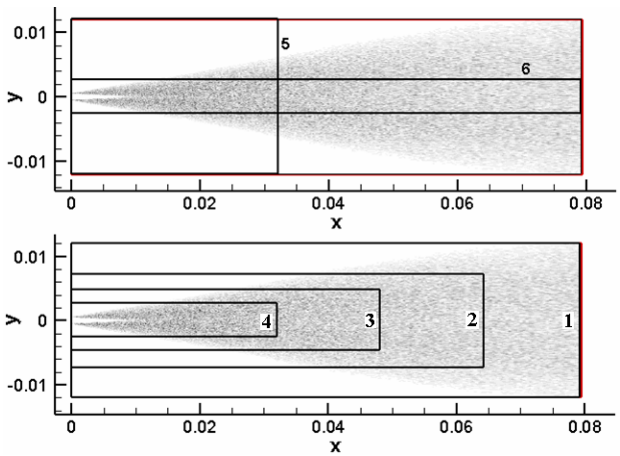

Figure 8. Integration zones of the flow field

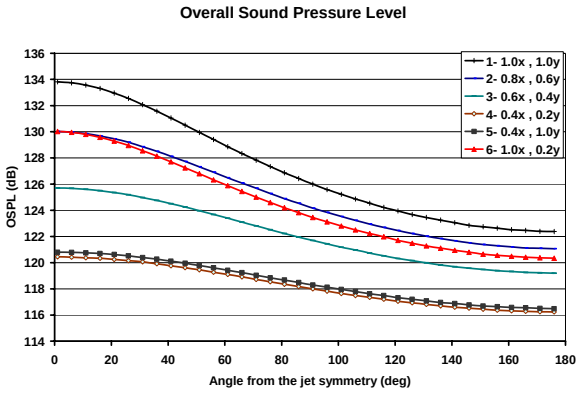

Figure 9. OSPL at 200D from the jet exit

Comparing the integration zones and their related OSPL, we find that regions containing large velocity fluctuations are most effective in sound propagated to the far field. For example regions 4 and 5 that have the same length with different width, almost produce the same amount of sound. Even though zone 5 is much larger than zone 4, however they both contain almost the same amount of velocity fluctuations in them. Hence, it is only important to integrate over the highly turbulent regions to compute the sound produced in jet flow.

In figure 10 the overall sound pressure levels from numerical computations are compared with the experimental data [10, 13] for a 2D cold jet at Mach number of 0.56. The OSPL on a half circle with the radius of 120D from the jet exit are presented.

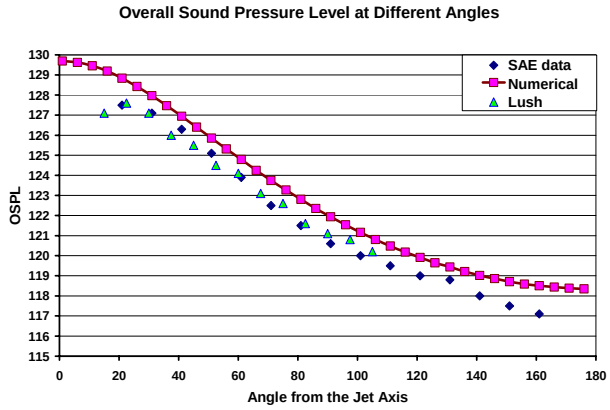

Figure 10. Comparison of the numerical results with the experimental data M=0.56 and |X|=120D (Lush [10] and SAE[13])

As shown in figure 10, the general trend in the numerical results is in reasonable agreement with the experimental data. The major difference between numerical results and experimental result is on predicting the maximum directivity angle of the jet. Numerical results show the maximum directivity to be at the jet axis (0 degree). There is no experimental data in vicinity of the jet axis because of the practical difficulties but it is known that the maximum directivity of the jet occurs at about 30 degrees from the jet axis.

There can be several reasons for this discrepancy. The CFWN method used here does not account for spatial structures that exist in real turbulent. As we know the directivity of the sound emitted from turbulent flows is due to large eddy structures existing in the flow. Hence, the discrepancy in the prediction of the maximum directivity can be expected. Also the size of the integral domain have to be large enough to contain all of the noise sources available in the flow, but as the CFD domain would become excessively large for far field calculations only a fraction of domain is considered here.

Conclusions

The stochastic method used here to simulate the velocity fluctuations satisfies the temporal properties of the turbulence. It also takes into account the intensity of turbulence flow. The calculated OSPL values and trends are in good agreement with the experimental results.

It seems that the combination of the CFWN method and Lighthill's volume integration is a good method for quick estimation of the overall OSPL with both reasonable computational speed and relatively good agreement with the experimental data.

This method is not as accurate as LES or DNS methods but as the LES or DNS data at the near field is not always available or too costly to generate for most geometries, this kind of stochastic methods are a good approach for cheap and quick estimates.

This method is not limited to free jet problems and can be used in other geometries too.

References

[1] Bailly C., Lafon P., and Candel S. (1997), *Subsonic and supersonic jet noise predictions from statistical source models*, AIAA journal. 35(11):1688–1696.

[2] Bodony D.J., Lele S.K., A Statistical Subgrid Scale Noise Model: Formulation, 9th AIAA/CEAS Aeroacoustics Conference and Exhibit 12-14 May 2003, Hilton Head, South Carolina

[3] Box, G.E.P, and Muller M.E. (1958), A note on the generation of random normal deviates, Annals Math. Stat, V. 29: 610-611.

[4] Chunhong H., Ahmadi G., (1999) Particle deposition in a nearly developed turbulent duct flow with electrophoreses, J. Aerosol Sci. Vol. 30, No. 6: 739-758.

[5] Dowling A.P., Hynes T.P., sound generation by turbulence , Europian Journal of Mechanics B/Fluids 23 (2004) 491-500

[6] Görtler, H. Berechnung Von Aufgaban der Freien Turbulnz auf Grund Eines Neunen Naherun Gsansatzes. Z.A.A.M. Vol 22, 1942

[7] Hirschberg A., Rienstra S.W., An Introduction to Aeroacoustics, July 2004.

[8] Lele S.K., Compact finite difference schemes with spectral-like resolution. J. Comput. Phys., 103:16–42, 1992.

[9] Lighthill MJ. (1952) On sound generated aerodynamically: I. General theory. Proc. R.Soc. London Ser. A 211(1107):564–587.

[10] Lush, P. A. (1971) Measurements of Subsonic Jet Noise and Comparison with Theory, Journal of Fluid Mechanics, Vol. 46, No. 3: 477-500.

[11] Lyrintzis A.S., Mankbadi R.R., Prediction of the Far-Field Jet Noise Using Kirchhoff's Formulation, AIAA J., 34(2) 413-416, 1996

[12] Morris P.J., Farassat F., Acoustic Analogy and Alternative Theories for Jet Noise Prediction, AIAA JOURNAL Vol. 40, No. 4, April 2002

[13] Society of Automotive Engineers, Gas Turbine Exhaust Noise Prediction, ARP 876C, Warrendale, PA, 1985.

[14] Thomson, D. J. (1987), Criteria for the selection of stochastic models of particle trajectories in turbulent flow, J. Fluid Mech. 180:529-556.

[15] Wang M., Freund J.B., and Lele S.K., Computational Prediction of Flow-Generated Sound, Annu. Rev. Fluid Mech. 2006. 38:483–512

[16] Zijnen, B.G., Van Der Hagge. (1958) Measurements of the Velocity Distribution In a Plane Turbulent Jet of Air. App. Sci. Res., Sect A, Vol 7.